



## Determination of High Frequency Earth Orientation Parameters by GNSS

Dzana Horozovic, Robert Weber

University of Technology, Vienna  
Department for Geodesy and Geoinformation

GEOWEB, Mostar, October 16th, 2017

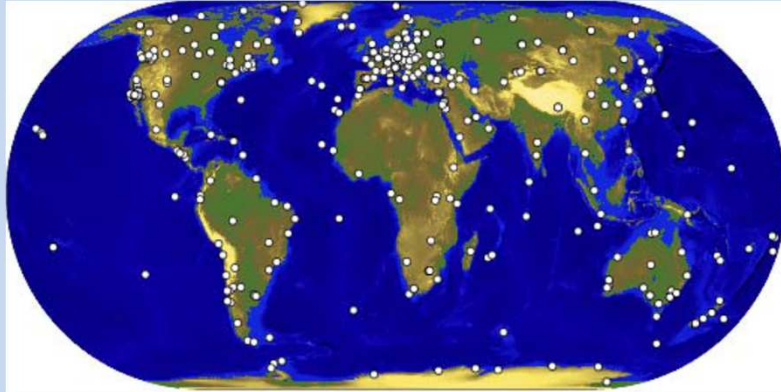
### Present day observation techniques

#### - VLBI and GNSS



In 2020 about 100 or slightly more GNSS satellites will be available to be utilized for ERP determination

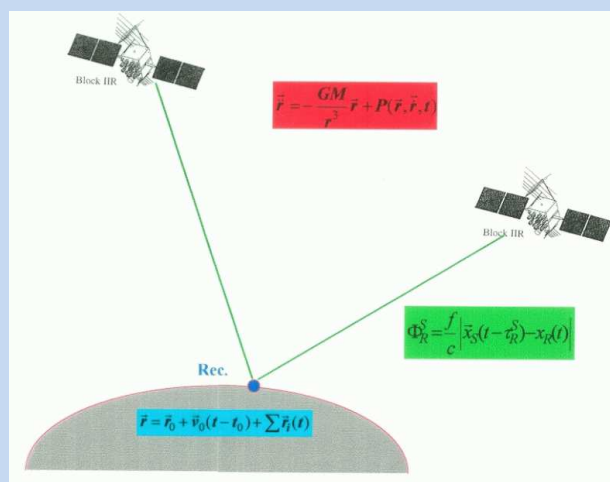
## Global Network for ERP/EOP Parameter Determination -> IGS-network



Our processing utilizes data from 130-170 global stations

### Relevant Reference Systems

Satellite Orbit Determination	->	Quasi-Inertial Frame
Site Positions	->	Earth-Fixed Frame
Observations	->	Frame invariant



## Relation: Celestial (Inertial) – Terrestrial System

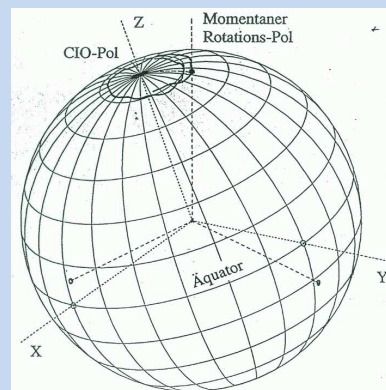
### Earth orientation parameters

are defined as rotation angles, which connect the Terrestrial co-rotating reference system with the Celestial inertial system by means of the relationship

$$r_c(t) = P N U X Y r_t(t).$$

P.....Precession  
 U.....Rotation (Parameter: UT1-UTC)  
 X,Y...Polar motion (Parameter: Pole coordinates x,y)  
 N.....Nutation (Parameter: Nutation offset  $\Delta\delta\varepsilon, \Delta\delta\psi$ )

These 5 Earth orientation parameters are linearly dependent (just 3 rotation angles theoretically independent)



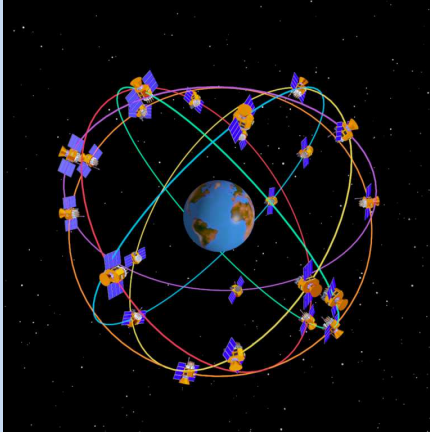
**ERPs: Polar Motion + (UT1-UTC) -> LOD, GPSUTC**  
**EOPs: ERPs+ Nutation Offsets**

## Agenda

- Introduction / Definition ERP/EOP
- Forcing of Rotation Variations (LOD, UT1-UTC)
- Project GNSS-EOP
- Geodetic versus Geophysical Excitations
- MGEX Data (GPS+Galileo)
- Amplitude Corrections to IERS Tidal Waves
- Comparisons to VLBI

6

### Accuracy of determined Parameters



GNSS allows for the determination of ERPs (ERPs) at the  $< 0.1 \text{ mas}/10 \mu\text{sec}$  level presupposed a global observation network and a complete satellite system

Dependent on temporal resolution of the parameters ->  
Low Frequency -> Periods  $> 1 \text{ day}$   
**High Frequency -> Periods  $\leq 1 \text{ day}$**

### Earth Rotation (UT1-UTC; LOD)



#### The Earth rotates – why ?

Linear and angular momentum of gases and dust particles of the proto-planetary disk; the angular momentum is transferred due to particle collision

### Definitions

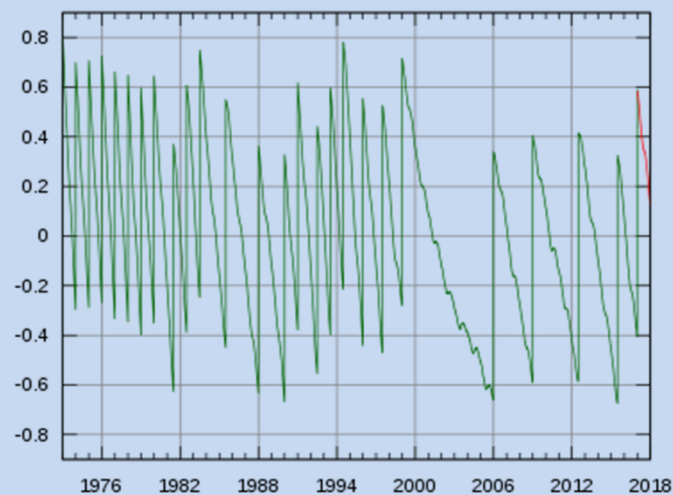
$$dUT1 = UT1 - UTC$$

Excess Length of Day  $\Delta LOD = LOD - 86400$  SI seconds

$$\Delta LOD = - \frac{dUT1}{dt}$$

$$\Delta T = TT (ET) - UT$$

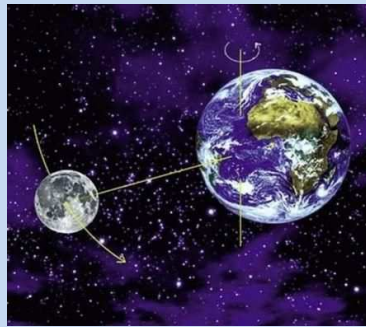
### dUT1= UT1 – UTC / Leap seconds



**Most recent leap-second Jan 1st , 2017 ; UTC-TAI = -37 s**

## Which effects can alter the angular velocity? (conservation of angular momentum)

Tidal effects  
(tidal brake, solid earth tides,...)



external forces

Variation of moments of inertia  
(wind, pressure, ocean currents)



internal forces

## Change in Length of Day due to Tidal Brake



### Estimate:

Assumption:  
Change in LOD per century:

$$\dot{\omega} = -1.6 \text{ ms/day / cy}$$

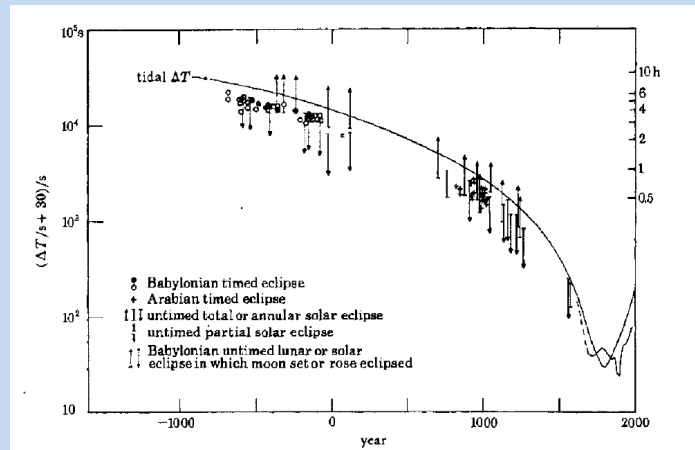
$$\Delta T = \dot{\omega} \frac{T^2}{2}$$

equates about 30s in T=1 cy

Equates about 8h in T=30 cy

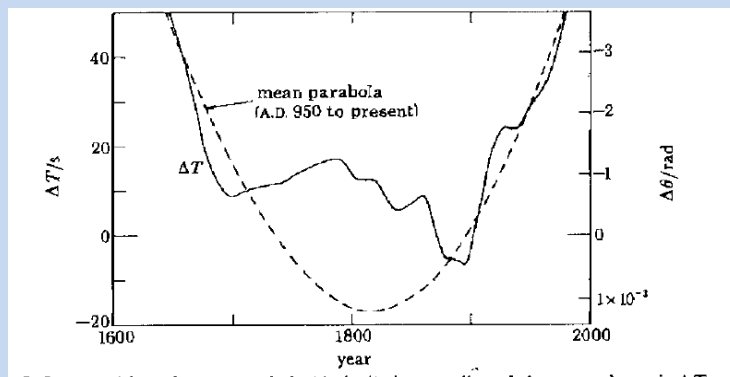
Proofed by LLR measurements: annual increase of lunar distance about 3.5 cm due to exchange of angular momentum --> angular momentum of system = constant

## Historic Change in Length of Day due to Tidal Brake $(\Delta T = TT (ET) - UT)$



Source: Stephenson, Morrison, 1984 (Trans. Royal Society, London)

## Change in Length of Day due to Tidal Brake

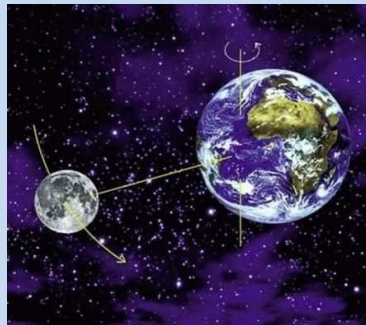


parabola corresponds to a tidally induced *apparent acceleration*  
of the Moon of  $-26'' \text{ arcsec}/\text{cy}^2$   
 $\Delta T = 0$  for  $t=1900.0$  is just per definition

Source: Stephenson, Morrison, 1984 (Trans. Royal Society, London)

## Which effects can alter the angular velocity?

Tidal effects  
(e.g. **tidal brake**)



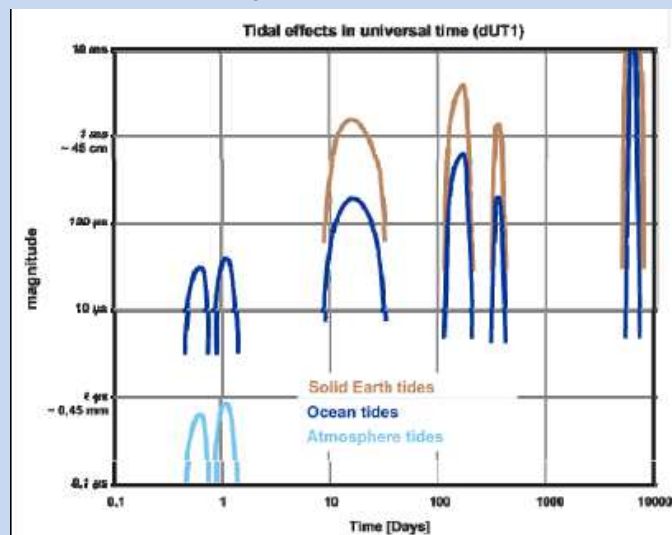
external forces

Variation of moments of inertia  
(**wind, pressure, ocean currents**)



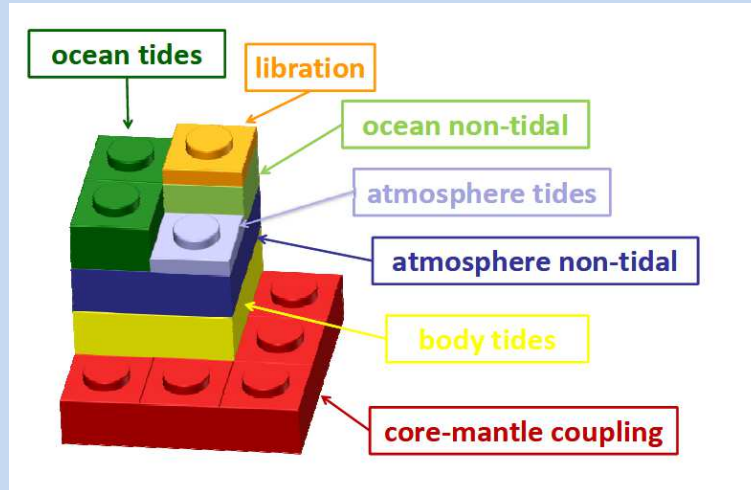
internal forces

## External and Internal Effects on Earth Rotation (Periods and Amplitudes)- Technical chart

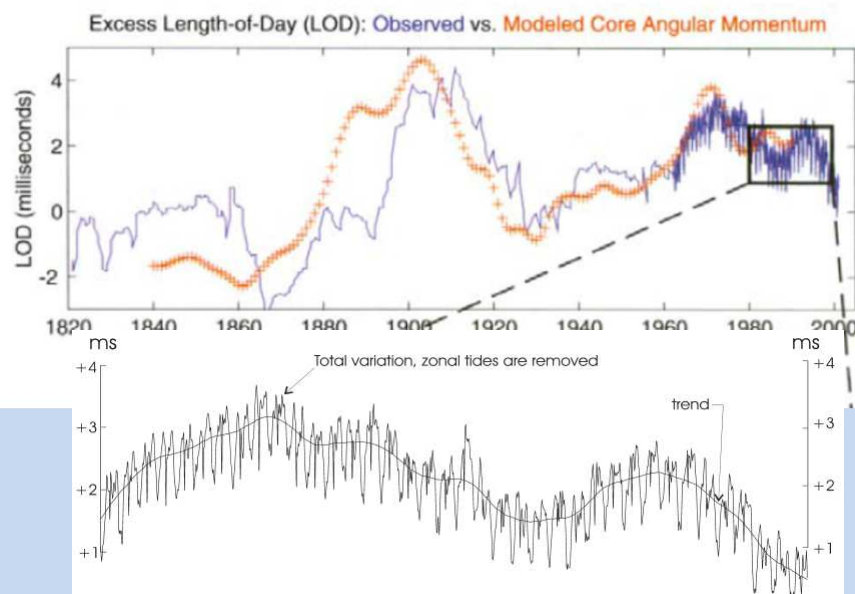




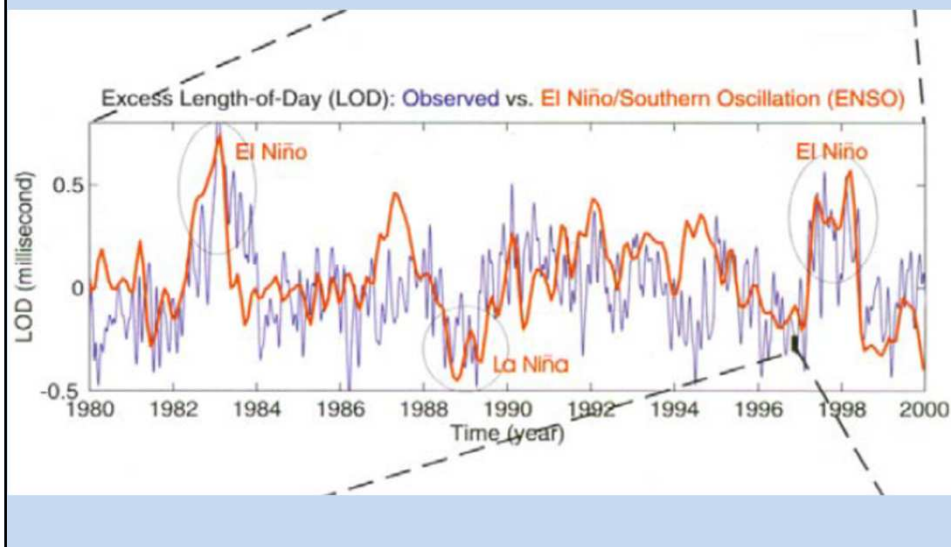
## External and Internal Effects on Earth Rotation (as Lego Cartoon 😊)



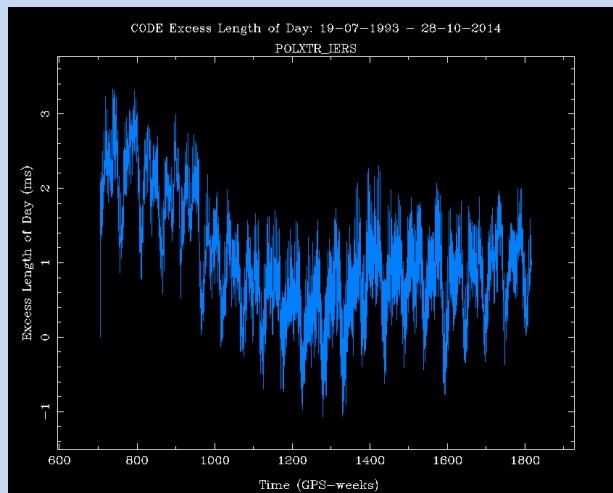
## Impact of Core-Mantle coupling on Earth rotation



## Impact of El Nino on Earth rotation



## $\Delta LOD$ 1993 – 2014



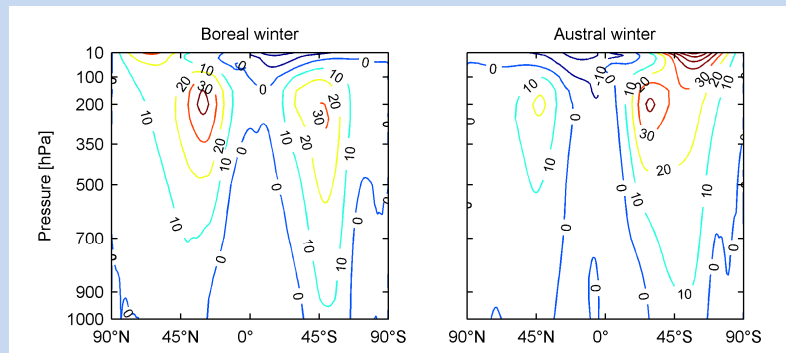
accuracy of LOD  
Estimates:  
 $\pm 10 - 15 \mu\text{s/day}$

Source: CODE Analysis Center

## Impact atmosphere (pressure, winds)



## How to determine Atmospheric excitation of $\Delta LOD$



Zonal mean of annual West-East-winds ( $u$ ) dependent on latitude  $\vartheta$  and pressure  $p$ . *Boreal winter*: D/J/F, *Austral winter*:

June/July/August

Integration of winds over

Volume unit:

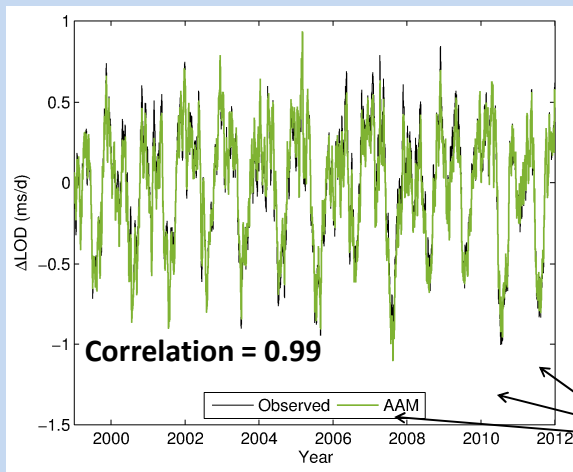
$$AAM^w = \frac{a^3}{g_{Am.}} \iiint u(\theta, \lambda, p) (\sin^2 \theta) d\theta d\lambda dp$$

22

## The whole story in equations 😊

<ul style="list-style-type: none"> <li>● Earth rotation observation             <ul style="list-style-type: none"> <li>▪ Polar motion of the CIP  <math>\hat{p}(t) = p_x(t) - i p_y(t)</math></li> <li>▪ PM of the rotation pole  <math>\hat{m}(t) = \hat{p}(t) - \frac{i}{\Omega} \frac{d\hat{p}(t)}{dt}</math></li> <li>▪ Excess length of day  <math>\frac{\delta LOD(t)}{LOD_0} = -\frac{d}{dt} dUT1(t) = -m_3</math></li> <li>▪ Geodetic excitation  <math>\hat{\chi}(t) = \hat{p}(t) + \frac{i}{\hat{\sigma}_{cw}} \frac{d\hat{p}(t)}{dt}</math>  <math>\chi_3(t) = \frac{\delta LOD(t)}{LOD_0}</math> ←</li> </ul> </li> </ul>	<ul style="list-style-type: none"> <li>● Geophysical Excitation             <ul style="list-style-type: none"> <li>▪ Equatorial effective angular momentum function (EAMF)  <math>\hat{\chi} = \frac{1.100 \cdot \hat{c}}{(C - A')} + \frac{1.608 \cdot \hat{h}}{\Omega \cdot (C - A')} = \hat{\chi}^{mass} + \hat{\chi}^{motion}</math></li> <li>▪ Axial EAMF  <math>\chi_3 = 0.748 \frac{c_{33}}{C_m} + 0.998 \frac{h_3}{C_m \Omega} = \chi_3^{mass} + \chi_3^{motion}</math> ↓</li> <li>▪ Geophysical excitation in terms of ERP  <math>\hat{p}(t) = e^{i\hat{\sigma}_{cw}t} \left( \hat{p}(0) - i\hat{\sigma}_{cw} \int_0^t \hat{\chi}(\tau) e^{-i\hat{\sigma}_{cw}\tau} d\tau \right)</math>  <math>\delta LOD(t) = \chi_3(t) \cdot LOD_0</math></li> </ul> </li> </ul>
---	--

### Prediction of Earth Rotation



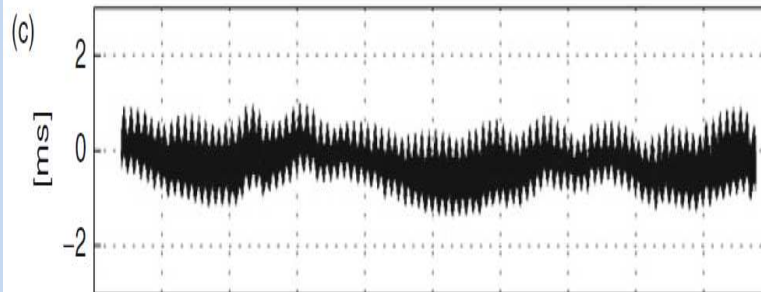
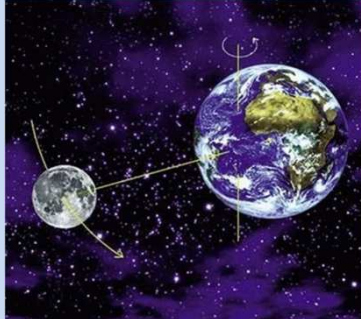
Comparison to Atmospheric Angular Momentum (AAM) calculated from numerical weather models

dominant annual Oscillation in AAM and ΔLOD

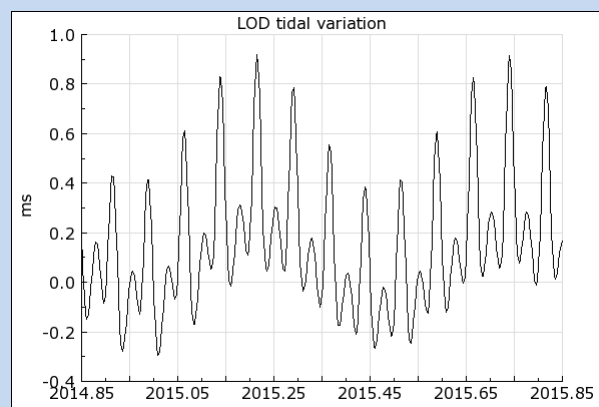
Correlation at Annual Period almost perfect

## Tides of Solid Earth (1960-2010)

Major periods:  
14 days, 28 days

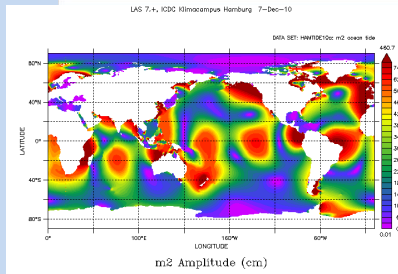
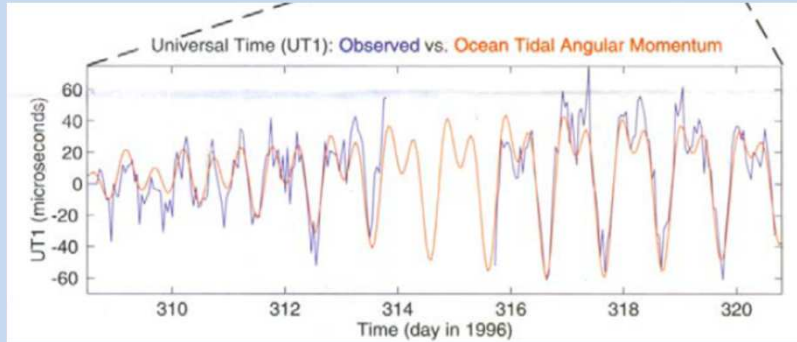


## Solid Earth Tides (zonal) in LOD 7.November 2014 - 7.November 2015



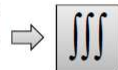
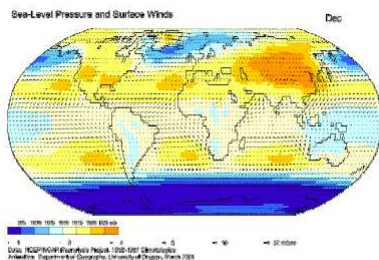
[http://hpiers.obspm.fr/eop-pc/models/UT1/UT1R\\_tab.html](http://hpiers.obspm.fr/eop-pc/models/UT1/UT1R_tab.html)

## Oceanic Tides (High Frequency contributions)

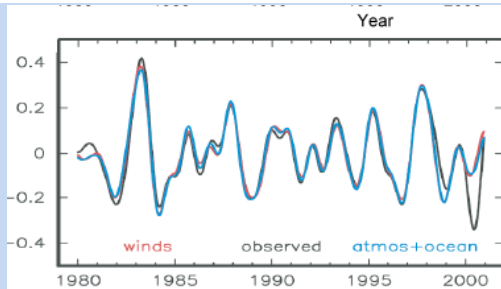


Major Periods: 24 hours, 12 hours

## Excitation is composed of contribution from Weather and Oceanic Models (AAM+OAM)



atmospheric excitation  
atmospheric angular momentum (functions)  
AAM(F)



Interannual LOD variations during 1980-2000 (Gross et al., 2004)

# GNSS – EOP: High frequency determination of the Earth Orientation Parameters by GNSS

TU-Vienna , Department for Geodesy and  
Geoinformation

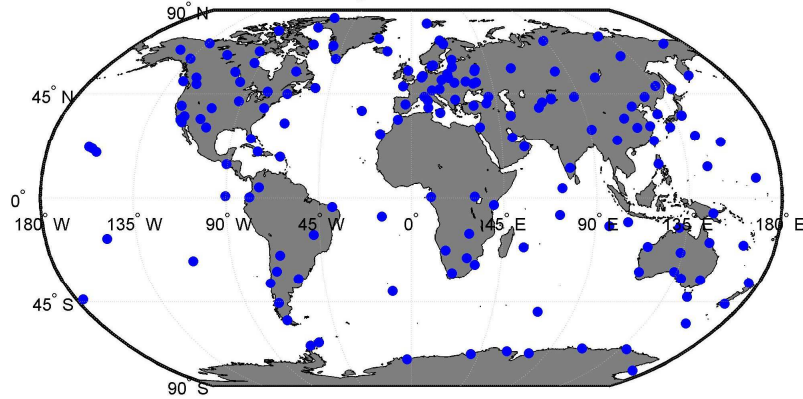
-  
Space Research Centre of the Polish Academy  
of Sciences at Warsaw, Department of  
Planetary Geodesy, Poland (SRC PAS)

## Project Goals

- Process high-accuracy GNSS Sub-diurnal ERPs based on GNSS observation data (GPS, GLONASS, Galileo)
- Compare results to corresponding VLBI data series
- Investigate potential of European VLBI to establish dUT1 time series comparable to results of a global VLBI network
- Calculate and compare geodetic and geophysical excitation functions (identify gaps between geodetic and geophysical excitation budget)
- Evaluate the potential of processing Galileo data in addition to GPS/GLONASS for the determination of EOPs (including nutation rates)
- Derive model for sub-diurnal tidal variations in Earth rotation and compare to IERS standard.

## Processing of sub-diurnal ERPs

### Global GNSS-EOP Network



Processed network: about 170 stations  
Reference Frame : ITRF2008  
NNR- Minimum Constraints Condition

GPS/GLONASS  
SRP: AIUB 9 Par. ECOM Model  
( 4 parameters constrained,  
5 parameters fitted)

## Processing of sub-diurnal ERPs

### Characteristics of the Solution

Campaign	Erpnet
Software	Bernese 5.2
Processing Period	Jan - May 2014 (doy002 - doy143) and ongoing
Type of Solution	1-Day/3-Day Solution
Observations	Phase and Code
A priori Orbits and EOP	IGS Final Products
Station Position and Station Velocities	ITRF2008
Absolute Antenna Model	IGS08
Station Network	174 Sites (NNR -> 81 stations)
Processing Mode	Double Differences
Ambiguity Resolution	QIF & WL/NL
Earth's Gravity	EGM2008_SMALL
Planetary Ephemerides	DE405
a priori Solar Radiation Pressure	C061001 (Code Model COD9801, Springer et al. 98)
Subdaily Pole Model	IRS2010XY (based on Ray 1994, XY - values)
Nutation Model	IAU2000R06
Solid Earth Tide Model	TIDE2000 (IERS2000)
Ocean Tides	OT_FES2004
Site - specific Correction for Ocean Tidal Loading	FES2004



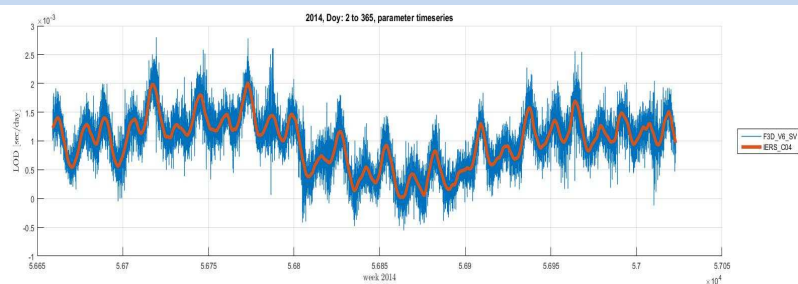
## Processing of sub-diurnal ERPs

### GNSS - ERP time series available for further investigations

- 1) Complete year 2008 (established at TU-Vienna)
- 2) Jan 1 – March 31, 2012 (provided by ETHZ, IGS re-processing)  
GPS+GLONASS
- 3) **Jan 2 – December 31, 2014 , established at TU Vienna**  
**GPS+GLONASS**
- 4) **Oct 1 – Dec 31, 2015 -> Galileo test**

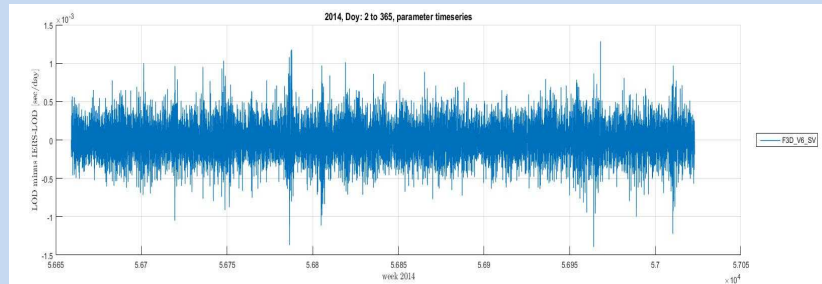
8

## LOD sub-daily time series 2014



Units: msec; Temporal resolution : 1h

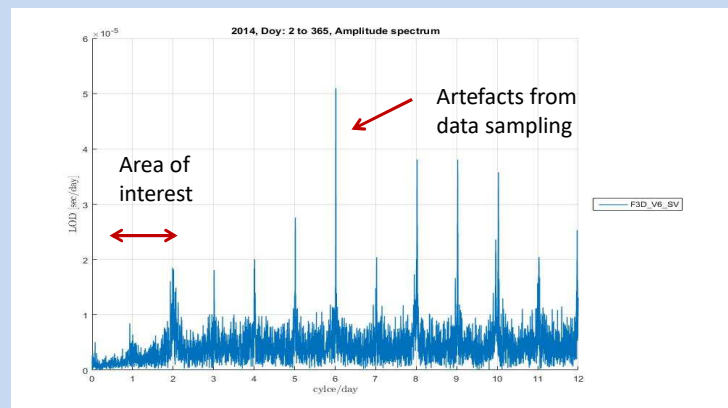
## LOD minus IERS-LOD



Estimated subdaily LOD – IERS C04 LOD (linear interpolated)

## (LOD – IERS subdaily LOD) Amplitude spectrum

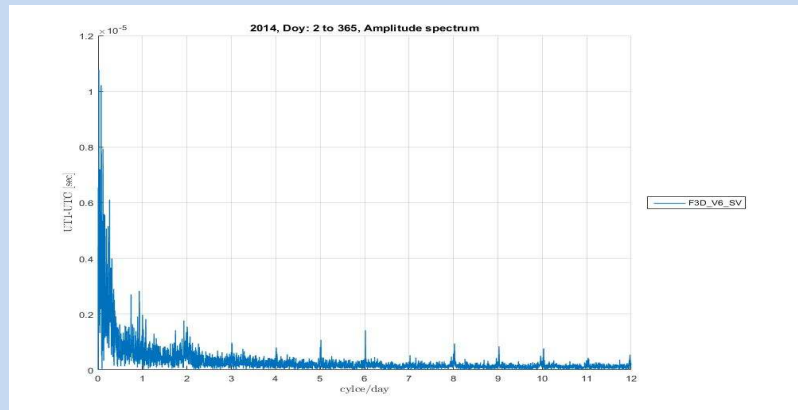
Units:  
10  $\mu$ sec



Spectra reveal remaining signals in the daily band up to a few  $\mu$ -sec /day and in the semi-diurnal band up to the 15  $\mu$ -sec/day level

-> confirmed later on in section model comparison to IERS

## (GNSS dUT1 – IERS subdaily dUT1) Amplitude spectrum



Spectra reveal remaining signals in the daily and semi-diurnal band of about 1-2  $\mu$ -sec. -> confirmed later on in section model comparison to IERS

## Investigations concerning GPS UT1 drift

It is well known that UT1-UTC parameters cannot be directly determined by satellite techniques. Also LOD is correlated with modelled orbital parameters (especially node). Therefore the integrated LOD (UT1GPS) exhibits a drift behaviour.

The UT1GPS drift compared to VLBI UT1 estimations is **mainly caused by an unmodeled out-of-plane component in the applied force model. This model deficiency can be directly related to imperfections of the Radiation Pressure Model and causes a twice per revolution effect.** As the SRP model improves, this drift decreases.

Various tests have been carried out how to minimize these problems by VLBI fixes.

### GNSS Integrated LOD + Nutation

According to [Rothacher 1999] the relation between LOD and nutation rates (old notation) and the first time derivatives of the orbital elements: (ascending node, inclination  $i$  and argument of latitude  $u_0$ ) reads:

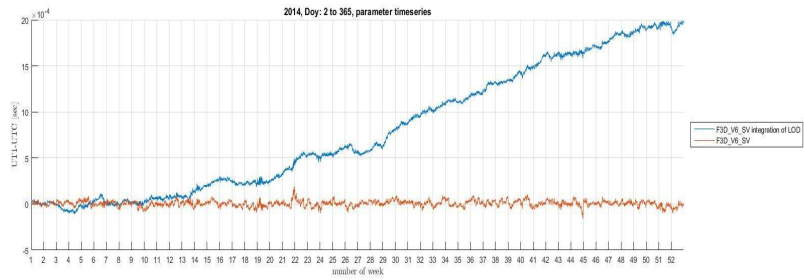
$$-LOD = -\left(\dot{\Omega} + \cos i \cdot \dot{u}_0\right) / \rho$$
$$\Delta \dot{\epsilon} = \cos \Omega \cdot \dot{i} + \sin i \sin \Omega \cdot \dot{u}_0$$
$$\Delta \dot{\psi} \cdot \sin \epsilon_0 = -\sin \Omega \cdot \dot{i} + \sin i \cos \Omega \cdot \dot{u}_0$$

From these equations we learn that the determination of LOD and the nutation rates with GNSS is possible as long as the orbital perturbations e.g. caused predominately by radiation pressure, are modelled sufficiently accurate.

### GPS UTC (integration of LOD)

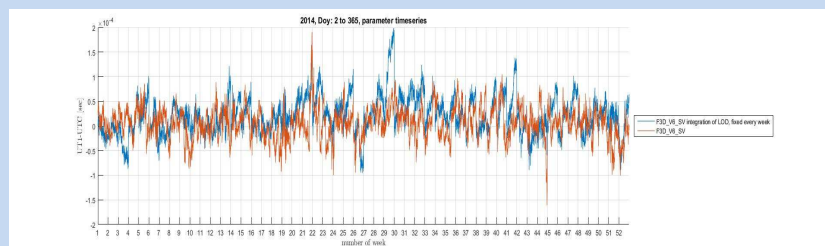
- The Bernese GNSS solution provides estimates of LOD and dUT1.
- The LOD values are integrated and compared with the raw dUT1 values in the following plots. Notice that both time series are referred to the IERS C04 values.
- There are three different versions of integration of LOD.
  - a) the LOD values are integrated and only fixed to zero (IERS C04 value) at the very first value,
  - b) the LOD values are integrated and fixed to zero every week,
  - c) the LOD values are integrated and fixed to zero every second week.

Version a) - UT1-UTC (integration of LOD)  
fixed to Jan 2, IERS dUTC



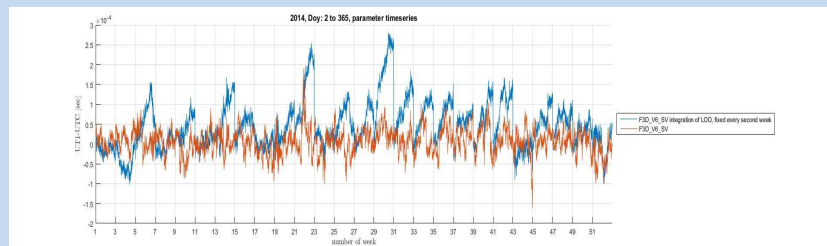
TUV- solution 3-days arcs;  
about 85 $\mu$ s drift in UT1-UTC over first 18 weeks  
but about 2ms over 52 weeks

UT1-UTC (integration of LOD), fixed every week  
Version b)



TUV- solution  
3-days arcs; drift in UT1-UTC about 100  $\mu$ s over 1 week  
-> once up to 200  $\mu$ s

## UT1-UTC (integration of LOD), fixed every second week – Version c)



TUV- solution

3-days arcs; drift in UT1-UTC about 150  $\mu\text{s}$  over 2 weeks

-> once up to 250  $\mu\text{s}$

## Processing of sub-diurnal ERPs

### Brief conclusions on LOD and GPSUT1 time series

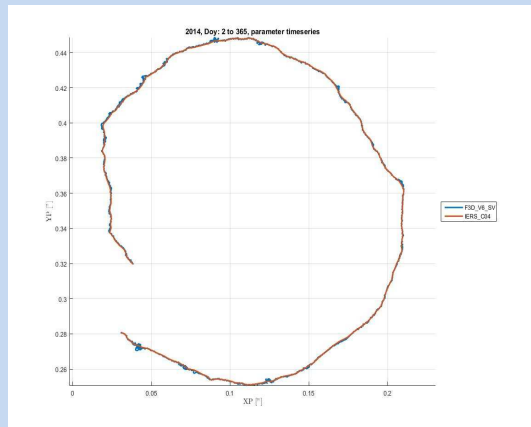
A few outliers in the TUV series are visible caused by occasional site data deficiencies. Series are processed several times to identify/correct network issues.

Spectra of LOD reveal remaining signals in the daily band up to a few  $\mu\text{-sec/day}$  and in the semi-diurnal band up to the 15  $\mu\text{-sec/day}$  level; the dUT1 series reflect remaining signals in the daily and semi-diurnal band of about 1-2  $\mu\text{-sec}$ .

Peaks in the spectra at  $1/n$  cycle/day are well-known artefacts. (8h term still under discussion).

The presented GNSSUT1 series are constrained to VLBI a priori values in various test cases.

## Polar Motion time series (2014)

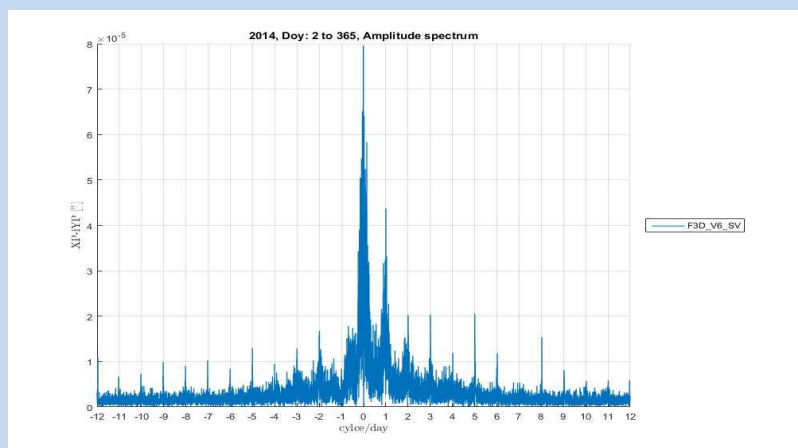


Blue:  
Estimates

Red: IERS-  
model

The retro-grade diurnal band was blocked in data processing of 1h- polar motion estimates- > nutation.

## GNSS residual XP - iYP Amplitude spectrum



Spectra reveal remaining signals in the daily and semi-diurnal band of about 0.02-0.04 mas.


-> confirmed later on in section Comparison to IERS model

## Processing of sub-diurnal ERPs

### Brief conclusions on processed polar motion series

X-pole and Y-Pole: Spectra reveal remaining **signals in the daily and semi-diurnal band of about 0.02-0.04 mas**. Major constituents belong to the prograde diurnal band while the semi-diurnal band (both prograde and retrograde) points to ocean-tide amplitude corrections  $< 0.02\text{mas}$ .

Remaining peaks in the spectra at  $1/n$  cycle/day are well-known artefacts.



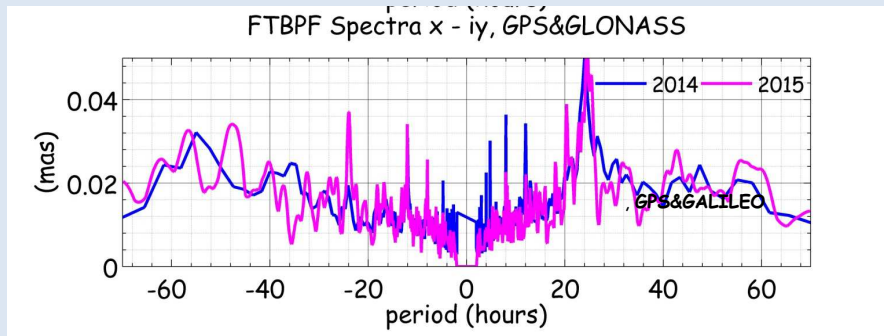
Space Research Centre  
Polish Academy of Sciences

Bartycka 18A, 00-716 Warsaw, phone.: +48 22 4966 200, fax: 022 840 31 31

## Geodetic and Geophysical Excitation Functions



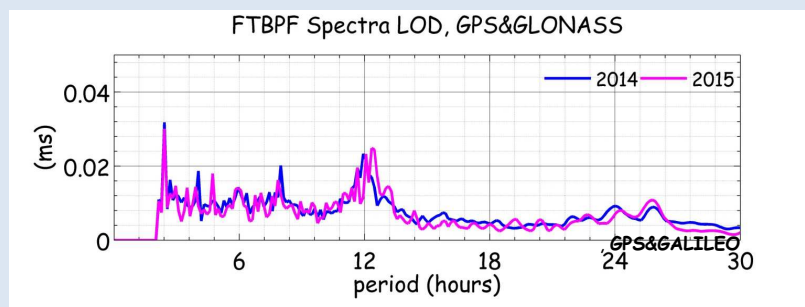
## Residual Spectra, X-iy : 2014,2015



2015 only 3 months

Comparison of FTBPF amplitude spectra of complex valued x-iy components determined in 2014 from GPS&GLONASS observations, and 2015 from GPS&GALILEO observations. Almost consistent in prograde diurnal band, Galileo series show larger differences in retrograde band.

## Spectra, LOD, 2014, 2015



Comparison of FTBPF amplitude spectra of LOD determined in 2014 from GPS&GLONASS observations, and 2015 from GPS&GALILEO observations.

## Geodetic excitation functions vs Geophysical Fluids

### Geophysical excitation functions

Atmospheric Angular Momentum (AAM) and Oceanic Angular Momentum (OAM) for 2012, 2014, 2015 data provided by Michael Schindelegger.

#### AAM Data

3-hourly AAM values were determined from the "assimilated state on pressure" stream of NASA's GEOS-5 Modern-Era Reanalysis for Research and Applications (MERRA).

#### OAM Data

3-hourly OAM values were determined from a barotropic ocean model that is a derivative of the model described in Schindelegger et al. (2016). It is forced by 3-hourly pressure and wind stress fields from the MERRA atmosphere and time steps the shallow water equations on a 30-minute grid.

## GeodeticExcitation Functions

The **usual method** of studying the perturbations of polar motion begins with computation of the excitation function from geodetic observations of x, y pole coordinates using the following formulas [WILSON 1985, BRZEZIŃSKI 1992]

$$\chi(t)^{GEOD} = \frac{ie^{\frac{-i\pi\Delta T}{T_{CW}}}}{\sigma_{CW}\Delta T} \left[ p\left(t + \frac{\Delta T}{2}\right) - e^{i\sigma_{CW}\Delta T} p\left(t - \frac{\Delta T}{2}\right) \right] \quad (1a)$$

$$\chi(t)^{GEOD} = \dot{p}(t) + i \frac{p(t)}{\sigma_c} \quad \text{or if a derivative is available} \quad (1b)$$

where the complex-valued excitation function  $\chi(t) = \chi_1(t) + i\chi_2(t)$  and the complex-valued polar motion  $p(t) = p_1(t) - ip_2(t)$ , with subscripts 1 and 2 corresponding to the x and y components, respectively.

The minus sign expresses the present convention according to which the y component of polar motion is measured positively toward the 90° W longitude, while the y axis of the TRS is oriented along the 90° E longitude. The complex-valued frequency of the Chandler wobble is described by  $\sigma_{cw} = 2\pi/T_{cw}(1 + i/2Q)$ . Here  $T_{cw}$  is the period and Q is the damping factors of the Chandler wobble.

UT1-UTC or LOD variations are linked to the axial component of the excitation function by the linear formula.

$$\chi_3^{GEOD} = -\frac{\Delta LOD}{86400s} + const \quad (1c)$$

## Spectra GEOD vs AAM + OAM (polar motion)

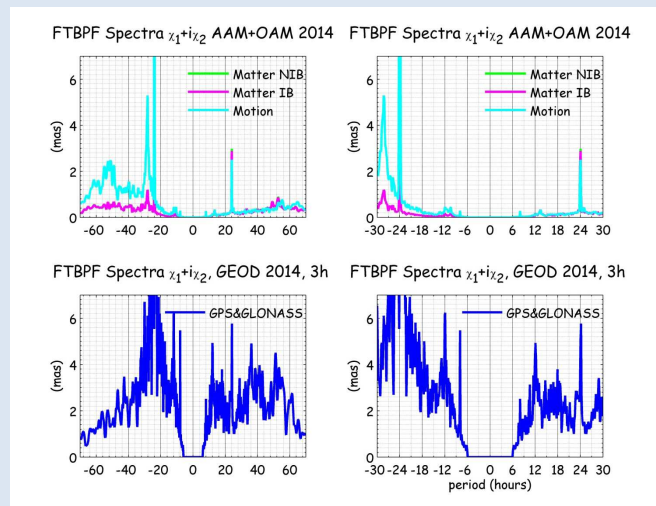
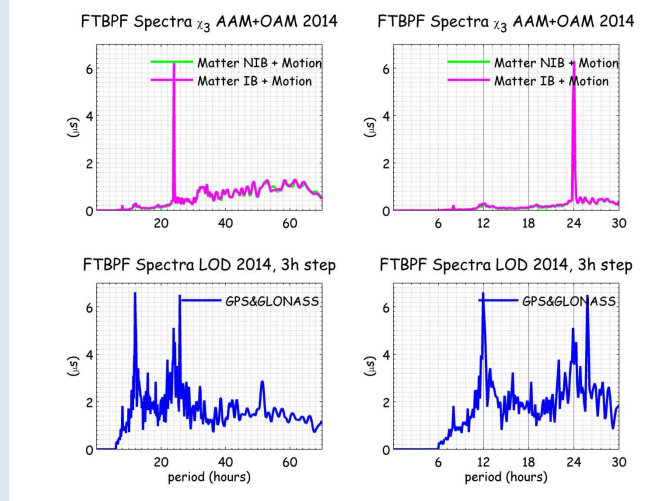


Figure 15 FTBPF spectra of  $\chi_1+i\chi_2$  complex-valued components of AAM+OAM separated into mass-non IB, mass IB plus and motion term (top panel) and geodetic excitation function determined for 2014 (bottom panel).

## Spectra LOD vs AAM + OAM



FTBPF spectra of  $\chi_3$  component of AAM+OAM separated into mass-non IB plus motion and mass IB plus motion term (top panel) and LOD determined for 2014 (bottom panel).

### Alternative method to calculate the geodetic excitation function and AAM+OAM by using a transfer function method (2 resonances)

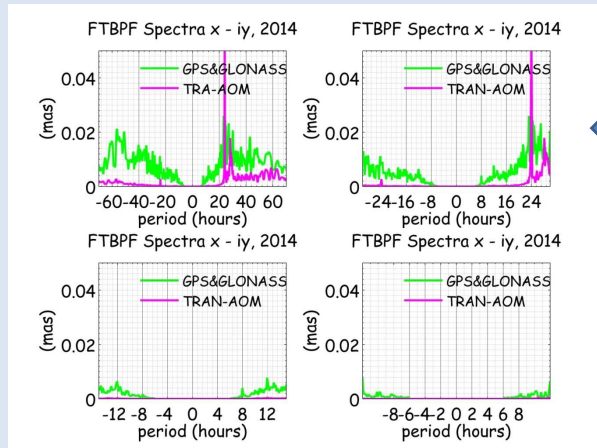
The equations below describing the transfer of polar motion to excitation of polar motion comprise of two parts which are the transfer functions of the matter (pressure, ocean bottom pressure) term  $T_p$  and motion (winds, ocean currents)  $T_m$  term.

$$sp(\sigma) = T_p(\sigma) s\chi^p + T_m s\chi^m(\sigma)$$

$$T_p = \sigma_c \left( \frac{1}{\sigma_c - \sigma} + \frac{a_p}{\sigma_f - \sigma} \right), \quad T_m = \sigma_c \left( \frac{1}{\sigma_c - \sigma} + \frac{a_m}{\sigma_f - \sigma} \right) \quad (3)$$

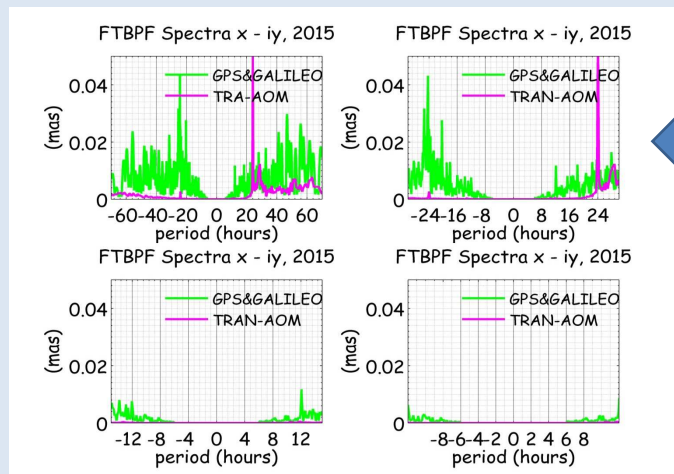
Where  $sp(\sigma)$  is the polar motion spectrum,  $s\chi^p$   $s\chi^m$  are spectra of the merged atmospheric plus oceanic excitation functions for matter and motion term, respectively,  $\sigma$  denotes the angular frequency,  $\sigma_f \approx -\Omega(1+1/430\text{days})$  the observed value of the Free Core Nutation (FCN) angular frequency of resonance,  $\sigma_c = \Omega/433$  days is the observed dissipation less value of the Chandler wobble resonance,  $\Omega = 7292115 \times 10^{-11} \text{rad/sec}$  is the mean angular velocity of the Earth's rotation, and  $a_p = 9.2 \times 10^{-2}$ ,  $a_m = 5.5 \times 10^{-4}$  are dimensionless constants.

**Comparison of the spectra of the geodetic excitation function and AAM+OAM by using a transfer function method (2015)**



Comparison of spectra of x-iy component of polar motion, (GPS+GLONASS) with the spectra obtained from atmospheric and oceanic excitation using the transfer function (TRAN-AOM)

**Comparison of the spectra of the geodetic excitation function and AAM+OAM by using a transfer function method (2015)**

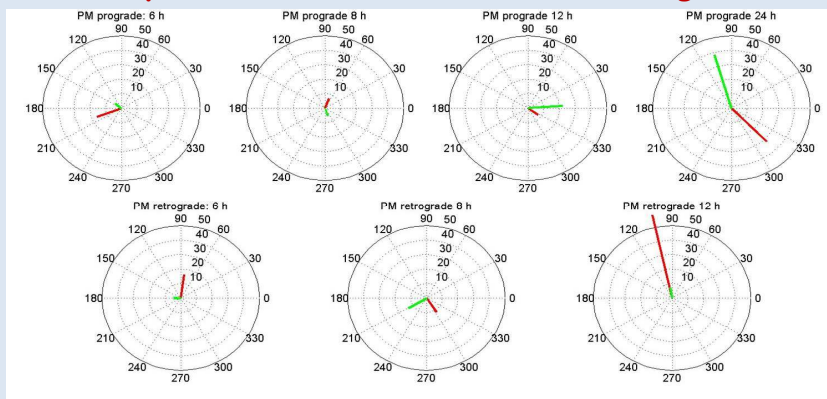


Comparison of spectra of x-iy component of polar motion GPS+GALILEO) with the spectra obtained from atmospheric and oceanic excitation using the transfer function (TRAN-AOM)

## Geodetic excitation functions vs Geophysical Fluids-Conclusions

- Analyses show considerable variability and a number of peaks in the spectral range below 12h.
- It is necessary to note that the amplitudes of spectra obtained using the transfer function **are still about one order smaller** than the spectra computed from the x and y component determined from the GNSS observations. The known geophysical excitations are much too small to explain the estimated ultra-rapid ERP variation amplitudes derived from GNSS as well as from VLBI data.

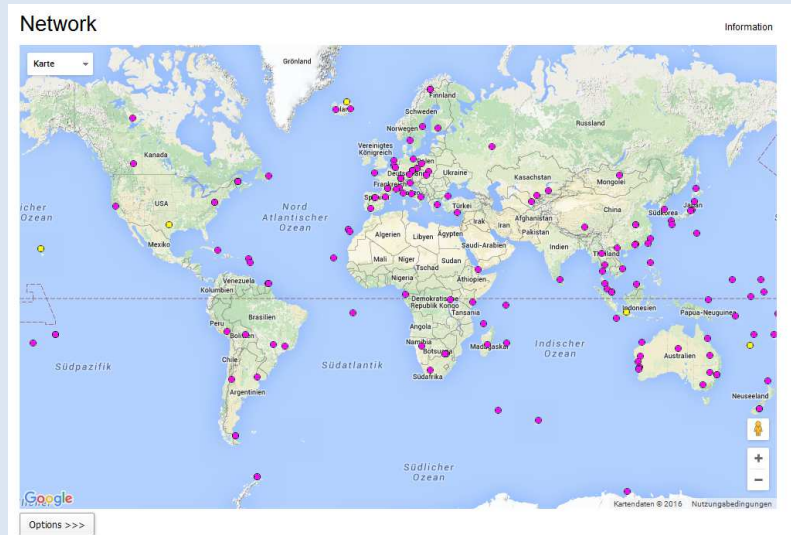
### Finally: Phase diagrams for polar motion. Units: $\mu\text{s}$ . Comparison : VLBI: in red, GNSS: in green



The phase diagrams of the (x-iy) component computed from the VLBI and the GNSS data are pretty **consistent in the case of the amplitudes** (except the prograde and the retrograde 6 hr and the retrograde 12 hr ).

However **the phases are quite different**, especially for diurnal prograde band.

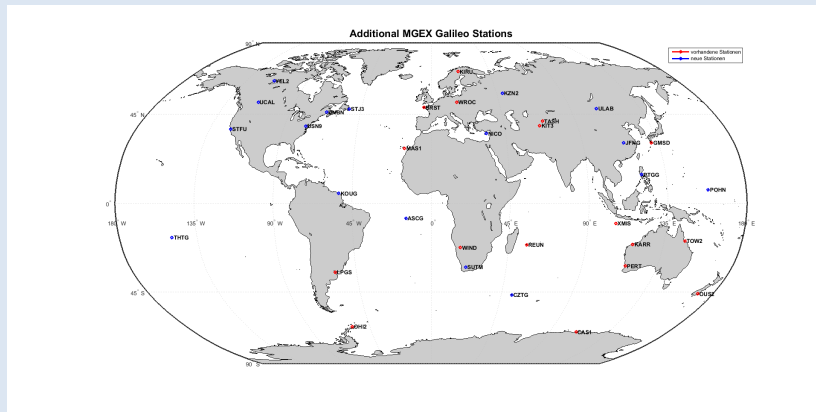
## Current MGEX Stations Network tracking also Galileo



### Observation-Data used for processing

- Data of about 80-100 stations available in MGEX CDDIS directories for 2015
- Considerable overlap to IGS network stations
- Establishing homogeneous GPS+Galileo Network from IGS+MGEX directories
- Observation data of **37 IGS MGEX** stations was retrieved mainly from the CDDIS directories. To establish a homogeneous GPS+Galileo Network we kept the network already processed in 2014 as a backbone, replaced 19 GPS+GLONASS data by GPS+Galileo data at sites with an also active multi-GNSS receiver (offering also Galileo data). In addition 18 new stations with GPS+Galileo data were added to the station pool.

## Additional MGEX Stations with Galileo observations



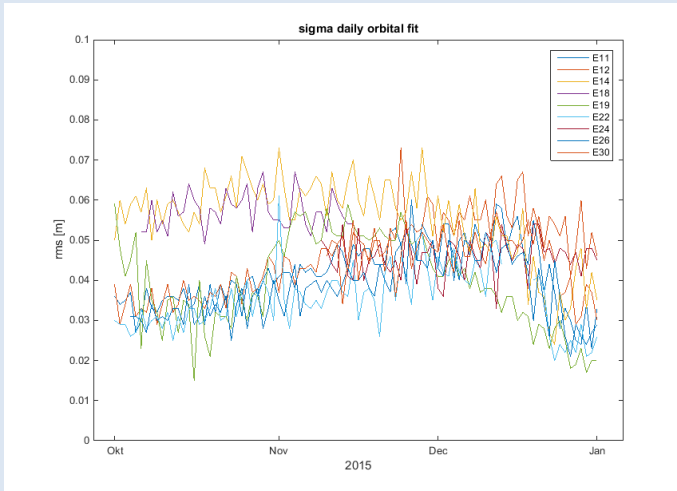
19 ,old' GPS+Galileo stations (red); 18 ,new' MGEX Galileo stations (blue)

## Galileo Orbit Fit

- Precise ESA GPS+Galileo orbits received for 2014/2015 as well as later on for Jan –June 2016
- Orbits cover a considerable amount of Galileo data ( $\geq 7$  sats ) from October 2015 onwards; before usually (4,5 sats)
- We agreed during last Technical Meeting in June to focus on Oct-Dec 2015 time period
- GPS+Galileo Orbits were fitted to the ESA orbit SP3 Files
- SRP: 5 parameters fitted on top of ECOM2 Model



### Galileo orbital daily orbital fit (October-December 2015)



Galileo fit  
about +/-4cm

GPS fit  
about +/- 2cm

**Note:** satellites  
E14,E18 in incorrect  
orbit  
See also E19

ECOM2 apriori + 5 parameters fitted (D0, Y0, X0, Ys, Xs)

### RMS of estimated EOP Parameters ( 3-days Solution) formal errors

RMS/Parameter	GPS	GPS&Galileo
RMS XP [arcsec]	0.00004	0.00004
RMS YP [arcsec]	0.00004	0.00004
RMS UT1-UTC [s]	0.000003	0.000002
RMS Delta Epsilon [arcsec]	0.00005	0.00005
RMS Delta Psi [arcsec]	0.00005	0.00005
RMS LOD [ms/D]	0.0089	0.0070



*Time derivatives of the Keplerian elements computed from the perturbing accelerations (R,S,W)*

$$\dot{i} = \frac{\cos u}{n a} W$$

$$\dot{a} = \frac{2}{n} S$$

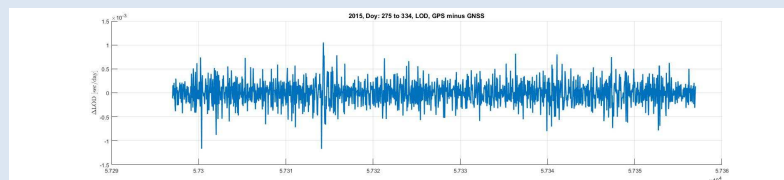
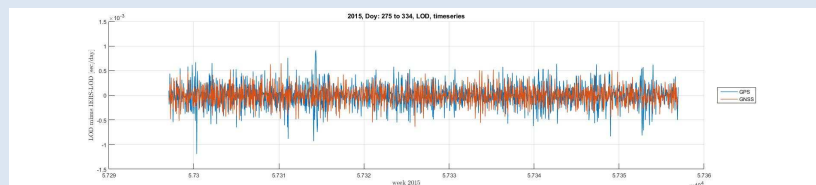
$$\dot{\Omega} = \frac{\sin u}{n a \sin i} W$$

$$\dot{u}_0 = \frac{2}{n a} R - \cos i \dot{\Omega} + 1.5 n/a (t-t_0) \dot{a}$$

Nutation rate estimates are very sensible to along-track (S) and out-of plane (W) deficiencies of the RPR-model (or correlated to RPR-model estimates) ; LOD is sensitive to out-of-plane RPR deficiencies ;

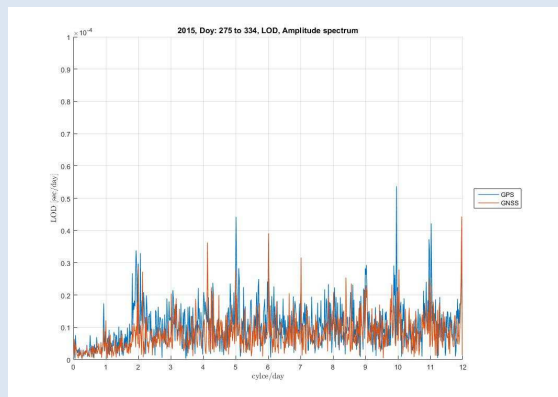
**Our approach for Galileo:** apriori model by Montenbruck, but solve-for parameters of ECOM

### LOD/ GPS versus GNSS



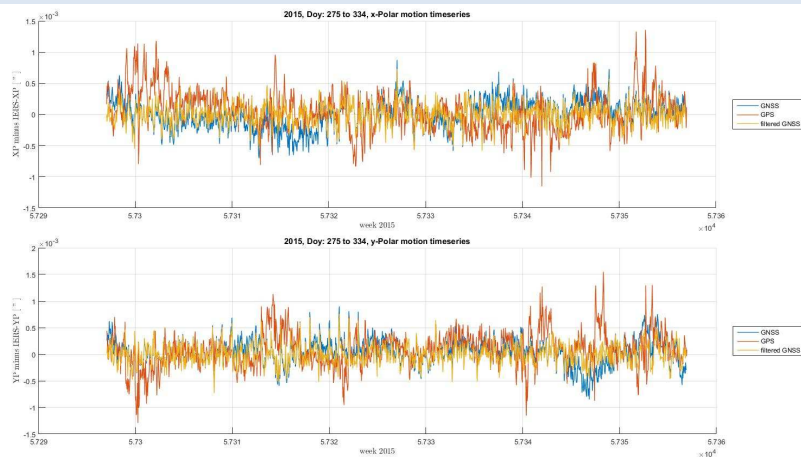
Differences at the 0.3 msec/day level

## LOD amplitude spectrum / GPS versus GNSS



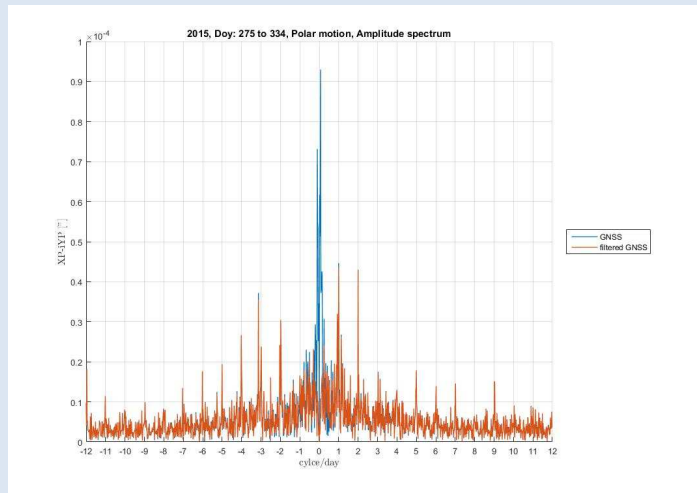
Noise floor of combined spectrum clearly smaller; artefacts remain  
Correction to IERS2010 in semi-diurnal band smaller than for GPS

## X,Y-Pole / GPS versus GNSS



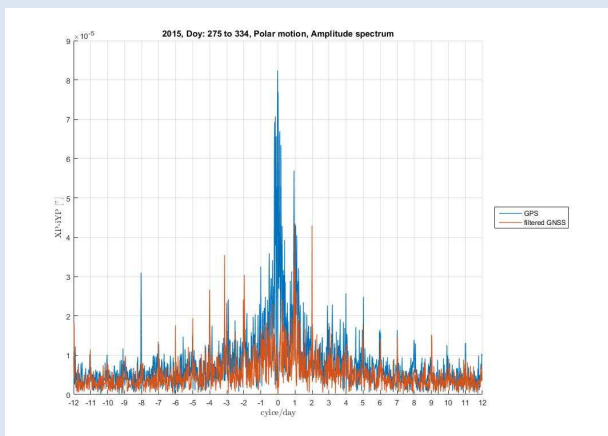
(red) GPS alone series – several outliers  
(blue) GPS+Galileo  
(yellow) – filtered GPS+Galileo series (**high-pass, 72 hours**)

## X,Y-Pole amplitude spectrum / GNSS versus filtered GNSS



Same results with exception at long wavelengths due to filtering

## X,Y-Pole amplitude spectrum / GPS versus filtered GNSS



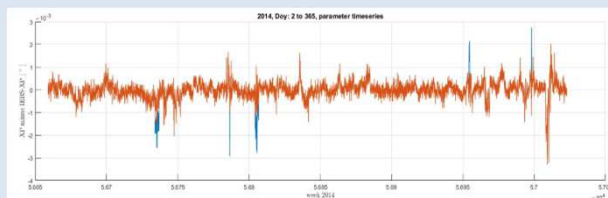
Clear improvement  
in noise level

as well as in  
residual amplitudes

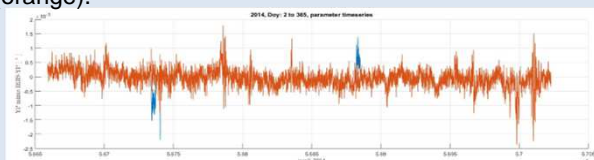
## Conclusions Galileo Tracking Data

- Combination of GPS+Galileo Data Processing has slightly improved the formal errors of the estimated ERPs
- Combination of GPS+Galileo Data Processing clearly reduces the noise level of ERP amplitude spectra and reveals smaller corrections to IERS2010 apriori model than GPS alone
- The full influence of Galileo to a combined GNSS ERP estimation could not be fully exploited as the Galileo observation data amount was still less than 10% compared to GPS
- Some of the improvements in the GPS+Galileo series might also refer to the more stable network in the southern hemisphere than used for GPS alone
- Due to the short data period (3 months 2015) and due to project time limitations we did not succeed in determining amplitude corrections for tidal waves with the GPS+Galileo series

## Comparison of estimated tidal waves to IERS model

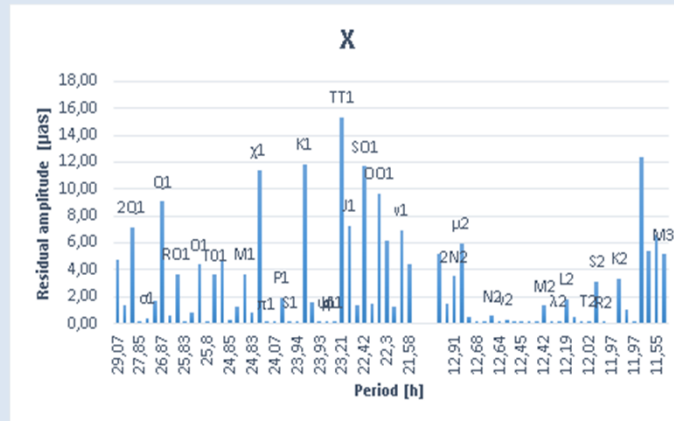


X-pole residuals with respect to IERS2010 model for period 2014. Original data series (blue); Corrected data series (orange).



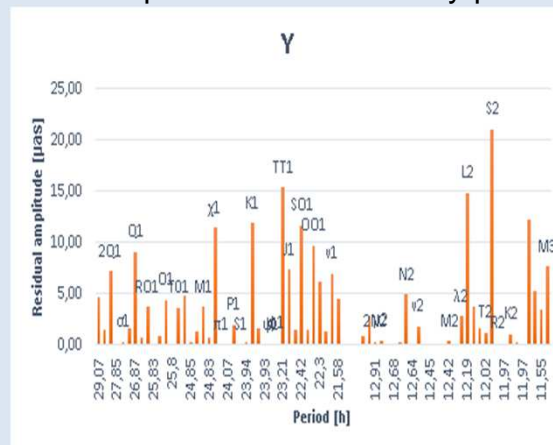
Y-pole residuals with respect to IERS2010 model for period 2014. Original data series (blue); Corrected data series (orange)

## GNSS-based Amplitude corrections to x-pole tidal terms



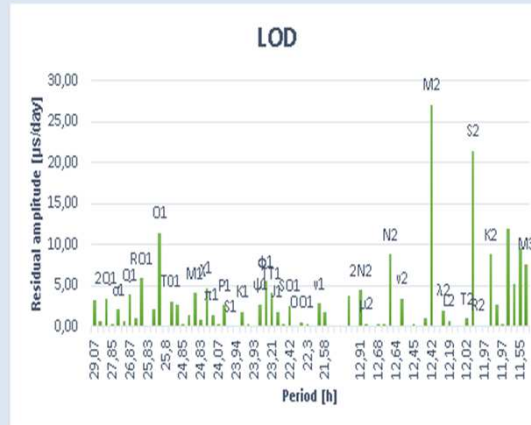
Corrections to the IERS Model up to 15 µas  
Major constituents in the diurnal band : Q1, Chi1, K1 ,T1,S01

## GNSS-based Amplitude corrections to y-pole tidal terms



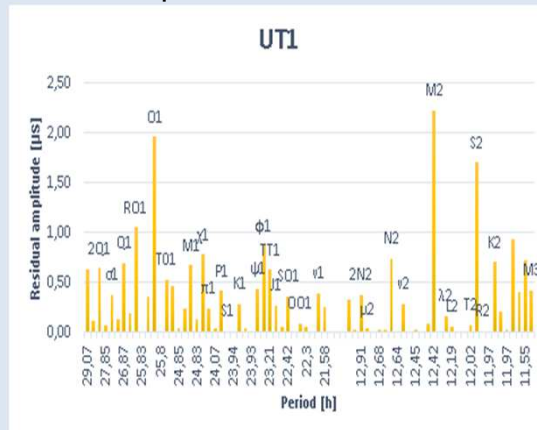
Corrections to the IERS Model up to 15 µas  
Major constituents in the diurnal band : Q1, Chi1, K1 ,T1,S1  
but also in the semidiurnal band L2, S2

## GNSS-based Amplitude corrections to LOD tidal terms



Corrections to the IERS Model up to 25  $\mu\text{s/day}$   
Major constituents in the semidiurnal band : M2, S2

## GNSS-based Amplitude corrections to dUT1 tidal terms

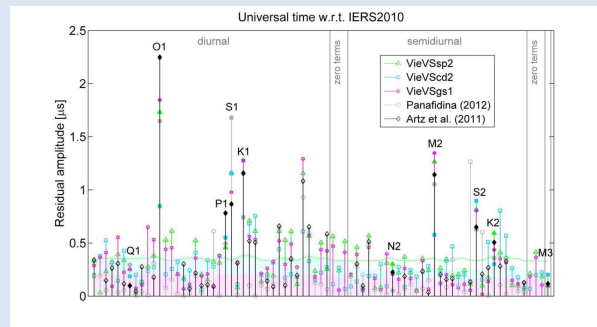


Corrections to the IERS Model up to 2  $\mu\text{s}$   
Major constituents in the diurnal (O1) and  
semidiurnal band : M2, S2

See  
comparison  
to VLBI  
corrections

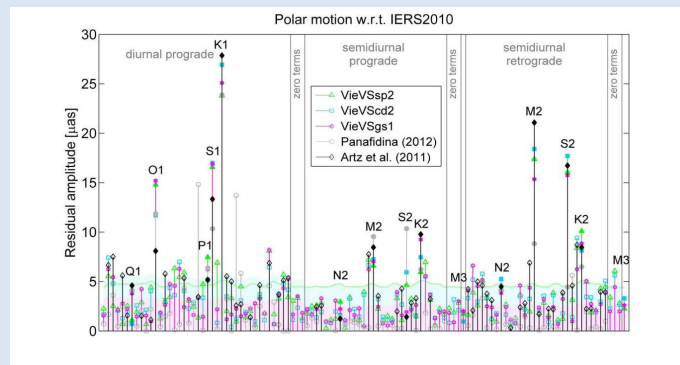
-> next slide

## UT1-UTC - Residual amplitudes VLBI – IERS2010XY



UT1-UTC - Residual amplitudes of 3 TUV-internal empirical VLBI solutions as well as 2 external VLBI solutions (Panafidina,2012; Artz et al. 2011); again O1, M2, S2

## Polar Motion - Residual amplitudes VLBI – IERS2010XY



Polar Motion - Residual amplitudes of 3 TUV-internal empirical VLBI solutions as well as 2 external VLBI solutions (Panafidina,2012; Artz et al. 2011)



## Conclusion on Model Corrections

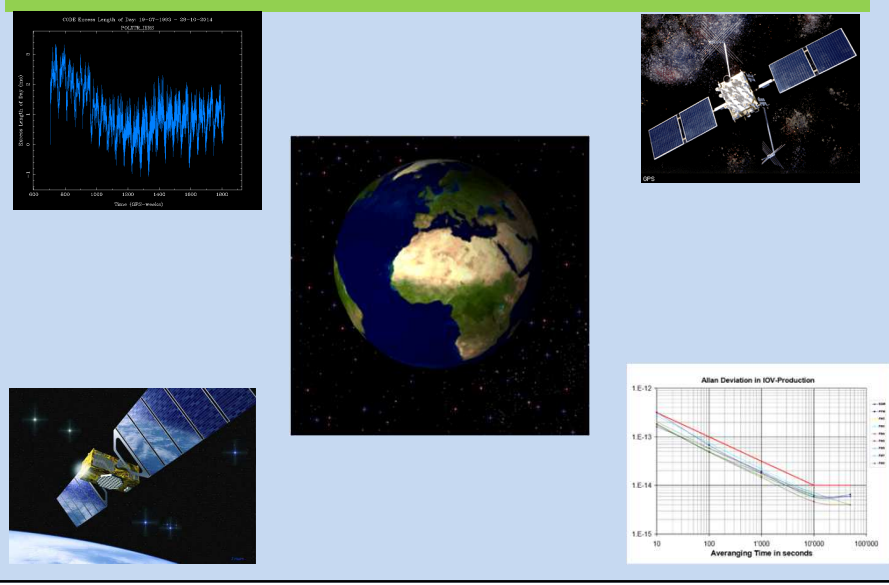
An inspection of the prominent peaks both in the VLBI solutions as well as derived from our GNSS 2014 solution reveals that

- The polar motion residual wave amplitudes of the VLBI solutions w.r.t. to the IERS2010 model are reasonable larger than those of the GNSS. Nevertheless O1, K1, S1, S2 remain to dominate the corrections in both solutions. On the other hand the M2 wave derived from GNSS data does not show any deviation from the IERS model numbers.
- The UT1 residual wave amplitudes of the VLBI and GNSS solutions w.r.t. to the IERS2010 model show a quite nice consistency. O1, M2 and S2 dominate both solutions identifying quite consistent deviations from the IERS model. The K1 wave correction visible in the VLBI solution does not show up in the GNSS solution. Also the S1 correction is quite larger for VLBI but the VLBI models deviate very strongly with respect to S1.

## Outlook

- We received further Precise Orbit Data for Galileo- and GPS satellites covering the period until mid 2016.
- New series have been calculated including a reasonable number of active Galileo satellites at least doubling the amount of Galileo data.
- RPR modelling for Galileo satellites is more demanding than for GPS.
- A working group has been established to improve the IERS subdaily pole model.

# Thank you for your attention

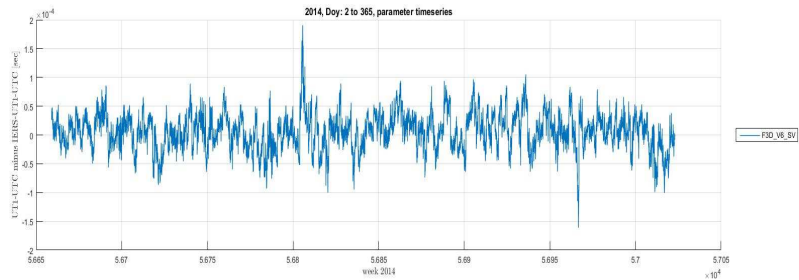


## Comparison of estimated tidal waves to IERS model

Diurnal variations	GSSS-EOPa	DD04-Diurnal-Tidal-Wavesa	TU results				IERS-coefficients											
			Arguments	UT1a	LODa	UT1a	LODa	UT1a	LODa									
DIPOLAR VARIATIONS	Tides	Y	I	F	D	Q	s	c	s	c	s	c	s	c				
	Y	18	-21	0	-2	-2	-2	0.38	5.61	-5.61	0.31	0	0.91	-0.91	-0.18			
	I	-2	18	-2	-2	-2	1.88	-1.00	1.00	1.82	0.11	0.61	-0.61	0.18				
	F	-2	-2	18	-2	-2	9.38	-5.11	5.11	9.38	0.28	3.41	-3.41	0.38				
	D	-2	-2	-2	18	-2	-2	-0.18	-0.71	0.71	-0.11	0.11	0.81	-0.81	0.18			
	Q	-2	-2	-2	-2	18	-2	-2	-0.48	-3.81	3.81	-0.51	0.51	4.21	-4.21	0.58		
	s	-2	-2	-2	-2	-2	18	-2	-2	1.78	6.61	-6.61	1.71	1.21	5.1	-5.1	1.28	
	c	-2	-2	-2	-2	-2	-2	18	-2	-2	9.01	-33.01	33.01	9.01	6.21	-26.31	-26.31	6.28
	s	-2	-2	-2	-2	-2	-2	18	-2	-2	0.28	-0.21	0.21	0.21	0.28	0.91	-0.91	0.28
	c	-2	-2	-2	-2	-2	-2	18	-2	-2	1.88	-1.00	1.00	1.82	0.11	0.61	-0.61	0.18
DIPOLAR VARIATIONS	Tides	Y	I	F	D	Q	s	c	s	c	s	c	s	c				
	Y	18	-21	0	-2	-2	-2	0.38	5.61	-5.61	0.31	0	0.91	-0.91	-0.18			
	I	-2	18	-2	-2	-2	1.88	-1.00	1.00	1.82	0.11	0.61	-0.61	0.18				
	F	-2	-2	18	-2	-2	9.38	-5.11	5.11	9.38	0.28	3.41	-3.41	0.38				
	D	-2	-2	-2	18	-2	-2	-0.18	-0.71	0.71	-0.11	0.11	0.81	-0.81	0.18			
	Q	-2	-2	-2	-2	18	-2	-2	-0.48	-3.81	3.81	-0.51	0.51	4.21	-4.21	0.58		
	s	-2	-2	-2	-2	-2	18	-2	-2	1.78	6.61	-6.61	1.71	1.21	5.1	-5.1	1.28	
	c	-2	-2	-2	-2	-2	-2	18	-2	-2	9.01	-33.01	33.01	9.01	6.21	-26.31	-26.31	6.28
	s	-2	-2	-2	-2	-2	-2	18	-2	-2	0.28	-0.21	0.21	0.21	0.28	0.91	-0.91	0.28
	c	-2	-2	-2	-2	-2	-2	18	-2	-2	1.88	-1.00	1.00	1.82	0.11	0.61	-0.61	0.18

For the complete tables see Technical Report DD04

## GNSS UT1-UTC minus IERS-dUT1 C04



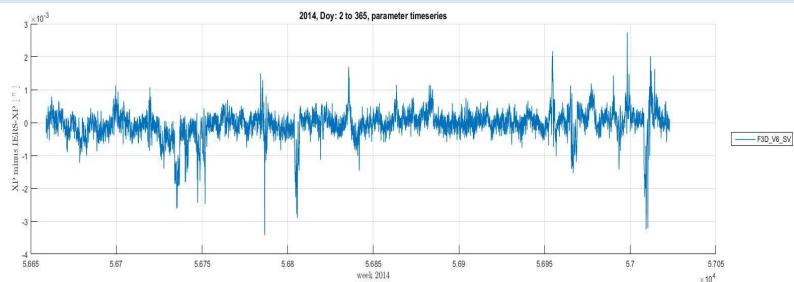
LOD integration starts from previous day 0h UT

14.09.2016

GNSS-EOP FR Meeting

14

## Subdaily GNSS X-pole minus IERS-X-pole (C04) Initial Approach



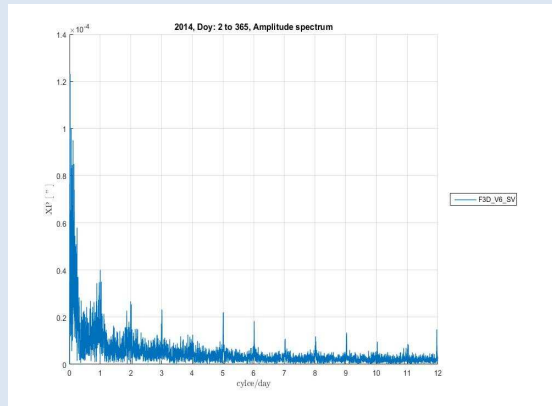
Differences at the 0.2 mas level + outliers  
Most outliers due to unstable south-hemisphere stations.  
See for corrected series in section on estimation of tidal waves

14.09.2016

GNSS-EOP FR Meeting

18

## GNSS X-pole – IERS subdaily X-pole model Amplitude spectrum



Spectra reveal remaining signals in the daily and semi-diurnal band of about 0.02-0.04 mas

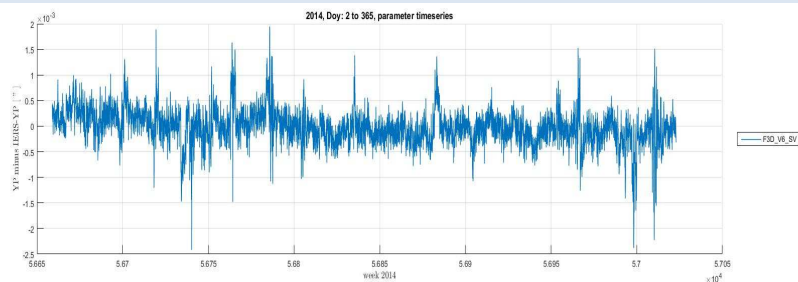
-> confirmed later on in section Comparison to IERS model

14.09.2016

GNSS-EOP FR Meeting

19

## Subdaily GNSS Y-pole minus IERS-Y-pole (C04) Initial Approach



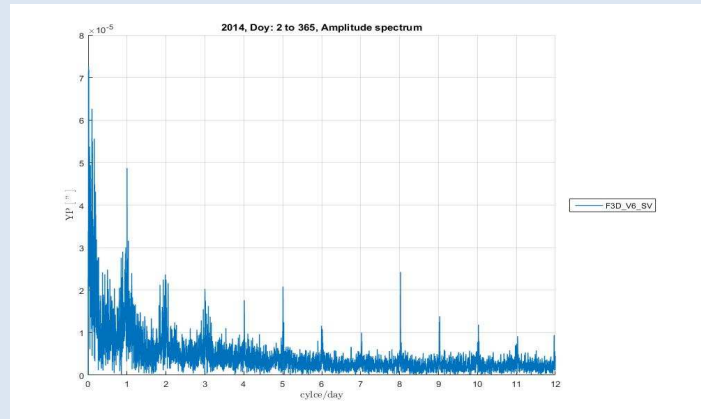
Differences at the 0.25 mas level + outliers

14.09.2016

GNSS-EOP FR Meeting

20

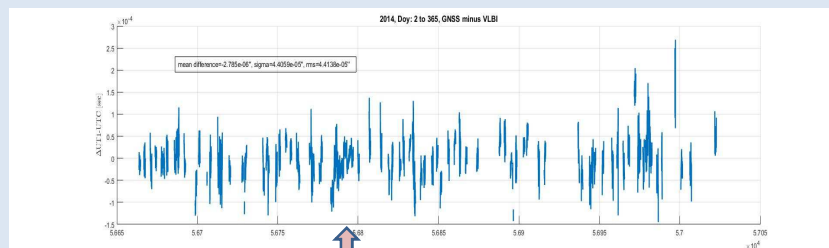
## GNSS Y-pole – IERS subdaily Y-pole model Amplitude spectrum



Spectra reveal remaining signals in the daily and semi-diurnal band of about 0.02-0.04 mas.

-> confirmed later on in section Comparison to IERS model

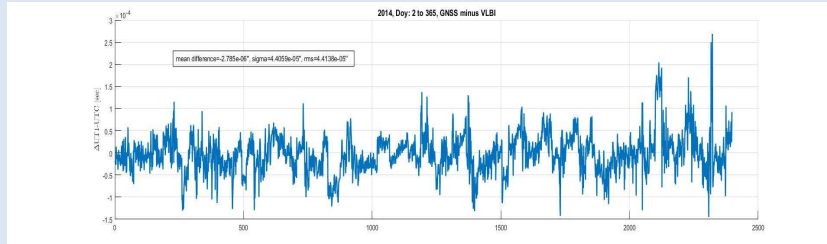
## GNSS minus VLBI, dUT1



CONT14

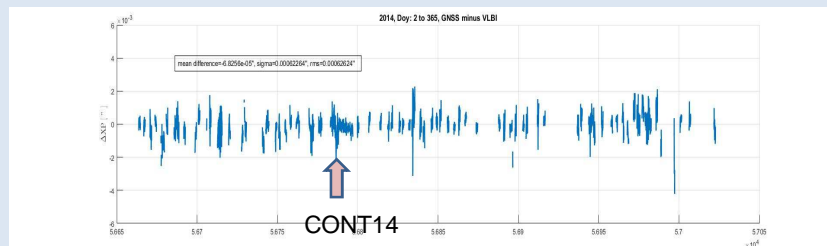
The graphic shows matching epochs and the gaps in the VLBI observations; the estimates correspond at the +/-40μs level.

## GNSS minus VLBI, dUT1



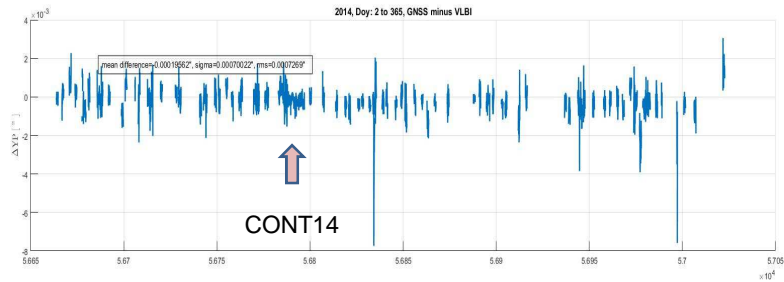
Same as above, but without gaps

## GNSS minus VLBI, X-pole



The graphic shows matching epochs and the gaps in the VLBI observations; the estimates correspond at the  $\pm 0.7$ mas level.

## GNSS minus VLBI, Y-pole



The graphic shows matching epochs and the gaps in the VLBI observations; the estimates correspond at the  $\pm 0.7$  mas level.

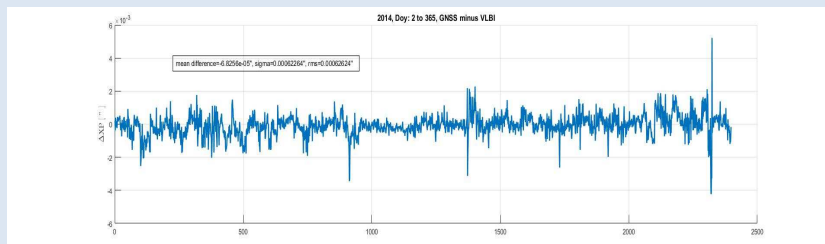
14.09.2016

GNSS-EOP FR Meeting

37

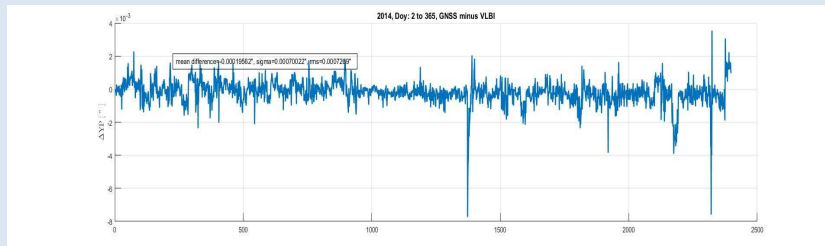
## GNSS minus VLBI, X-pole

All corresponding epochs are plotted in a sequence



## GNSS minus VLBI, Y-pole

All corresponding epochs are plotted in a sequence



VLBI data series were passed to SRC PAS for detailed investigations

14.09.2016

GNSS-EOP FR Meeting

39

## GNSS Nutation

According to [Rothacher 1999] the relation between LOD and nutation rates (old notation) and the first time derivatives of the orbital elements: (ascending node, inclination  $i$  and argument of latitude  $u_0$ ) reads:

$$-LOD = -\left(\dot{\Omega} + \cos i \cdot \dot{u}_0\right) / \rho$$

$$\Delta \dot{\epsilon} = \cos \Omega \cdot \dot{i} + \sin i \sin \Omega \cdot \dot{u}_0$$

$$\Delta \dot{\psi} \cdot \sin \epsilon_0 = -\sin \Omega \cdot \dot{i} + \sin i \cos \Omega \cdot \dot{u}_0$$

From these equations we learn that the determination of LOD and the nutation rates with GNSS is possible as long as the orbital perturbations e.g. caused predominately by radiation pressure, are modelled sufficiently accurate.



## nutation rates processing 2014 (GPS alone)

### Characteristics of the Solution

Campaign	Erpnet
Software	Bernese 5.2
Processing Period	Jan - May 2014 (doy002 - doy143) and ongoing
Type of Solution	1-Day/3-Day Solution
Observations	Phase and Code
A priori Orbits and EOP	IGS Final Products
Station Position and Station Velocities	ITRF2008
Absolute Antenna Model	IGS08
Station Network	174 Sites (NNR -> 81 stations)
Processing Mode	Double Differences
Ambiguity Resolution	QIF & WL/NL
Earth's Gravity	EGM2008_SMALL
Planetary Ephemerides	DE405
apriori Solar Radiation Pressure	C061001 (Code Model COD9801, Springer et al. 98)
Subdaily Pole Model	IERS2010XY (based on Ray 1994, XY - values)
Nutation Model	<b>IAU2000R06</b>
Solid Earth Tide Model	TIDE2000 (IERS2000)
Ocean Tides	OT_FES2004
Site - specific Correction for Ocean Tidal Loading	FES2004



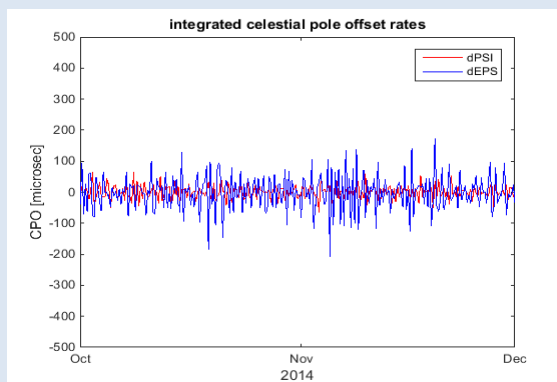
14.09.2016

GNSS-EOP FR Meeting

66

## Integrated nutation rates (1)

Nutation rates were processed for 2014, testing various constraints on the apriori model



Series w.r.t. IAU2000R06 model

Period: October - November 2014

Nutation model 'loosely' constrained to 0.1 mas

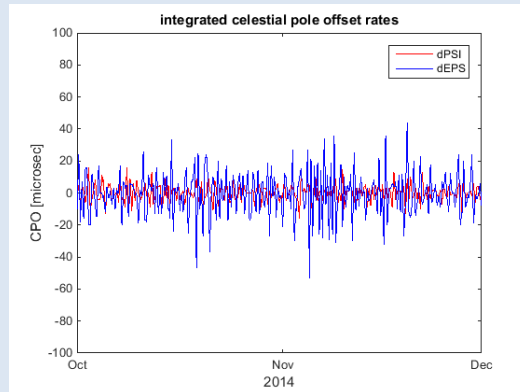
Rate estimates every 6 hours, retro-grade diurnal polar motion blocked

14.09.2016

GNSS-EOP FR Meeting

67

## Integrated nutation rates (2)



Series w.r.t. IAU2000R06 model  
 Period: October - November 2014  
 Nutation model, constrained to 0.05 mas  
 Rate estimates every 6 hours, retro-grade diurnal polar motion blocked

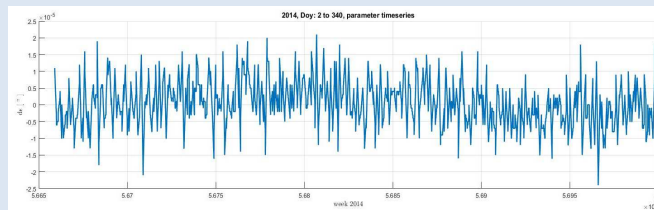
14.09.2016

GNSS-EOP FR Meeting

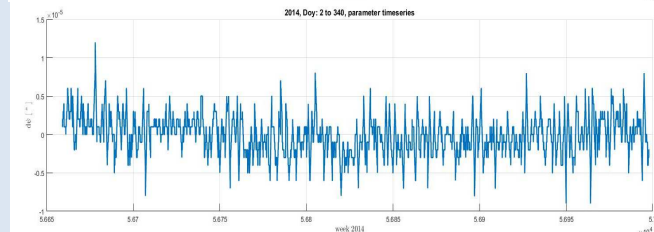
68

## Nutation rates per day (complete year 2014)

obliquity / deps



longitude / dpsi



Series w.r.t. IAU2000R06 model, Period: January- December 2014  
 Nutation model, constrained to 0.05 mas  
 Rate estimates every 24 hours, retro-grade diurnal polar motion blocked

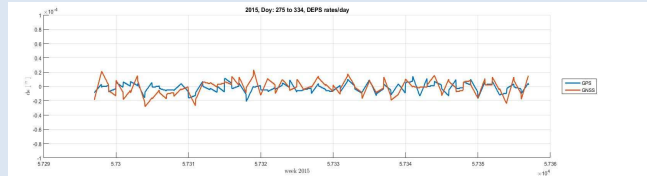
14.09.2016

GNSS-EOP FR Meeting

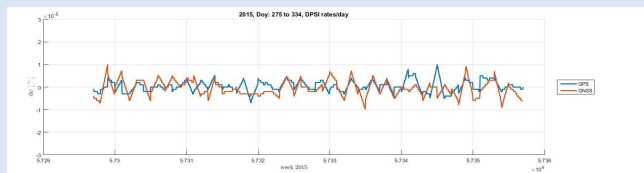
100

## Galileo versus GPS Nutation rates per day (October-November 2015)

obliquity / deps



longitude / dps



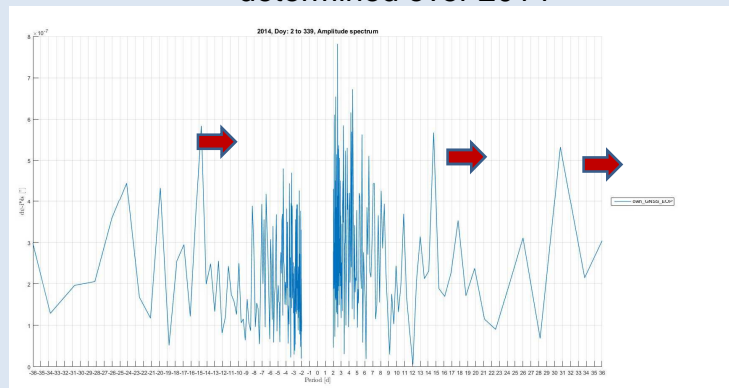
Series w.r.t. IAU2000R06 model, Period: October- November 2015  
 Nutation model, constrained to 0.05 mas  
 Rate estimates every **24 hours**, retro-grade diurnal polar motion blocked

14.09.2016

GNSS-EOP FR Meeting

101

## Amplitude spectrum of the nutation rate estimates determined over 2014



Spectrum between 2-36 days both in the prograde and retrograde band. Distinct peaks well above the noise level are visible at 14 days and close to 30 days. No visible correction to 7.11 days term. Up to now no nutation wave amplitude corrections were determined

14.09.2016

GNSS-EOP FR Meeting

102

## Short Characterization of AAM and OAM data

**AAM and OAM data provided by Michael Schindelegger -**

### **AAM Data**

3-hourly AAM values were determined from the "assimilated state on pressure" stream of NASA's GEOS-5 Modern-Era Reanalysis for Research and Applications (MERRA). (-> 2015 MERRA2)

### **OAM Data**

3-hourly OAM values were determined from a barotropic ocean model that is a derivative of the model described in Schindelegger et al. (2016). It is forced by 3-hourly pressure and wind stress fields from the MERRA atmosphere and time steps the shallow water equations on a 30-minute grid.

14.09.2016

GNSS-EOP FR Meeting

51

## **GNSS vs VLBI-Conclusions**

The phase diagrams of the (x-iy) component computed from the VLBI and the GNSS data are pretty consistent in the case of the amplitudes (except the prograde and the retrograde 6 hr and the retrograde 12 hr ). However the phases are quite different, especially for diurnal prograde band.

Oscillations of the excitation functions determined from the GNSS observations dominate spectra in the spectral range up to 10 hours while those computed from the VLBI became larger below 4 hours.

22.11.2016

GNSS-EOP – GSAC Presentation

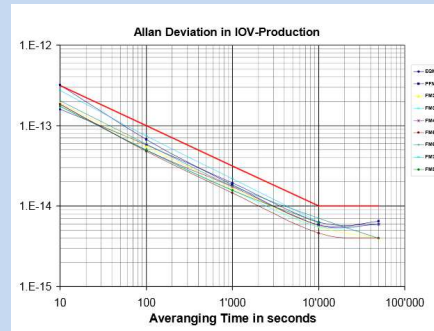
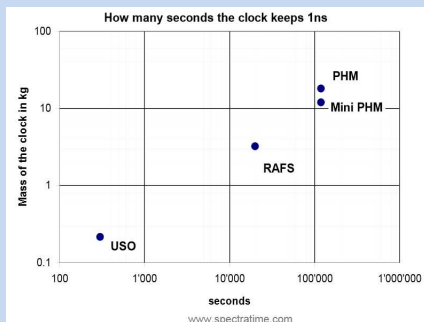
37

## Zukunft der Uhrqualität

Eine Uhr läuft umso stabiler je schneller ihr ‚Pendel‘ schwingt -> Pendelfrequenz => Resonanzfrequenz

a) GALILEO Hydrogen Maser

**Frequenz Stabilität Galileo –Wasserstoffmaser besser als  $10 \text{ E-14}$   
Resonanzfrequenz 1.4 GHz**



Graphics – Source : Spectra Time Company (2009)

## GNSS vs VLBI Comparison

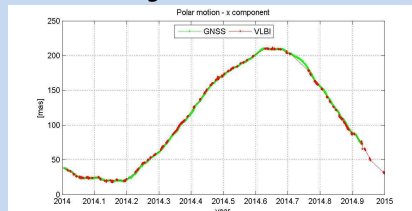
In the context of this project also a data series of ERPs with hourly resolution derived from all available 24h VLBI sessions has been established at TUV. This data series covers the period from begin of 2012 until end of 2015.

In contrast to GNSS, 24h VLBI sessions are not carried out on a daily basis, which causes gaps in the series of up to a few days.

We focused on the comparison between the VLBI and GNSS data for polar motion for the year 2014, as this period is the only year when we had both types of data available.

The following data sets provided by TUV were investigated:

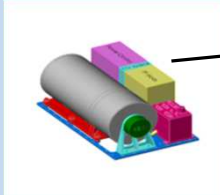
- GNSS (GNSS\_EOP2014.txt)
- VLBI (total\_val\_detailed.txt)



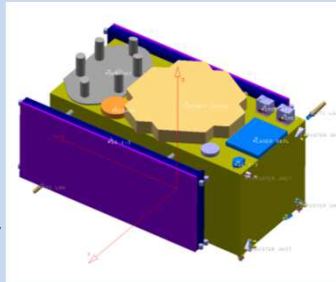


### On-board Atomic Clocks

**Passive Hydrogen Maser**  
18 Kg mass  
70 W power



**Rubidium Atomic Frequency Standard**  
3.3 Kg mass  
30 W power



**Navigation P/L:**  
130 Kg / 900 W

#### Types of Atomic Clocks

##### Rubidium Clock

- Cheaper and Smaller
- Better short-term stability (European RAFS  $s=5.0 \cdot 10^{-14}$  at 10000 sec)
- Subject to larger frequency variation caused by environment conditions

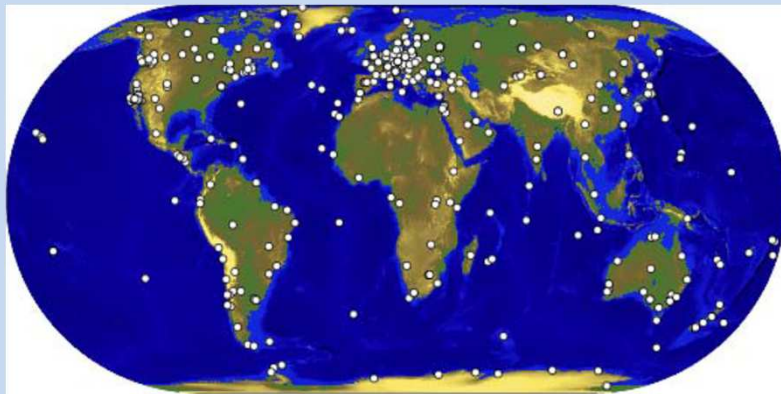
##### H-Maser Clock

- outstanding short-term and long term frequency stability ( $10^{-15}$ )

##### Caesium Clock

- Better long-term stability ( $10^{-14}$ )
- shorter life time
- not used in Galileo

### Commonly used observation data: IGS-network



Our processing utilizes data from 130-170 global stations